Polar cap area and boundary motion during substorms

M. Brittnacher, M. Fillingim, and G. Parks

Geophysics Program, University of Washington, Seattle, Washington

G. Germany

CSPAR, University of Alabama in Huntsville, Huntsville, Alabama

J. Spann

NASA Marshall Space Flight Center, Huntsville, Alabama

Abstract. The area of the polar cap as a function of local time and substorm phase was measured using images from the Polar Ultraviolet Imager (UVI) for different interplanetary magnetic field (IMF) orientations during three substorms in January 1997. We measured changes in the polar cap area and motion of the poleward and equatorward boundary of the auroral oval. It was found that the polar cap boundary is strongly influenced by thinning of the oval, decrease in polar cap structures, the poleward expansion of the substorm at midnight, and the fading of luminosity below the instrument sensitivity threshold. Generally, these effects dominate over the latitudinal motion of the auroral oval at its equatorward edge. A new feature is that the polar cap region clears of precipitation during the substorm growth phase, which expands the size of the polar cap but is not necessarily related to an expansion of the open flux region. Another finding is that the increase in polar cap area prior to onset can be independent of the strength of the southward IMF component. For one case the polar cap area increased while the southward component of the IMF was 0 ± 0.5 nT. These observations have strong implications for models that use the polar cap area to estimate the magnitude of energy storage in the lobe magnetic field and loss during substorms.

1. Introduction

The area of the polar cap, the region poleward of the auroral oval where the magnetic flux tubes are considered to be open with respect to the interplanetary magnetic field (IMF), has been of great interest since changes in its size have a fundamental connection with magnetospheric dynamics during substorms. Reconnection substorm models rely on magnetic field from the solar wind that has merged with Earth's magnetic field as a source of energy [e.g., *Russell and McPherron*, 1973]. The storage and release of magnetic flux in the tail lobes is thought to cause the polar cap to expand and contract, respectively [*Siscoe and Huang*, 1985]. According to these models, the polar cap area is a fundamental quantity. For example, the polar cap area as determined by auroral images has been used to indicate the changes in energy storage and release during the growth and expansion phases [*Frank and Craven*, 1988; *Baker et al.*, 1994, 1997].

The open flux region that defines the polar cap region is not presently an experimental observable instantaneously on a global scale. In practice, the poleward boundary of the auroral electrojets [*Akasofu and Kamide*, 1975], auroral luminosity [*Meng et al.*, 1977; *Craven and Frank*, 1987; *Frank and Craven*, 1988; *Lassen and Danielson*, 1989; *Elphinstone et al.*, 1990; *Kamide et al.*, 1998], ion and electron particle boundaries [*Makita et al.*, 1985; *Troshichev et al.*, 1996], and, more recently, magnetic fluctuations [*Gary et al.*, 1998] have been used to determine the polar cap boundary and thereby infer changes in the polar cap size. Satellite observations have revealed that the polar cap area increases during the substorm growth phase and decreases following the substorm onset, but the phenomenon is rich with complexity, and there are different explanations of the physics involved. By analyzing particle boundaries from the Defense Meteorological Satellite Program (DMSP) in situ measurements, *Meng and Makita* [1986] suggested that the polar cap area expanded during southward IMF and that the maximum area of the polar cap was achieved near the time when the AE index was the largest. They also indicated that the increase in the distance between the boundaries of the polar cap along the noon-midnight and dawn-dusk

meridians during southward IMF was not equivalent. *Kamide et al.* [1998] later expanded on this point by using Dynamics Explorer 1 (DE 1) images to show that the solar wind can have a direct influence on the dawn and dusk boundaries of the polar cap, while changes in the boundary near midnight were attributed to unloading processes during substorm expansion. *Frank and Craven* [1988] also used DE 1 images to suggest that the IMF controls the expansion of the polar cap during the substorm growth phase and that the area promptly decreases with the onset of the expansion phase, presumably because of loss of lobe flux. *Murphree et al.* [1991] questioned the interpretation that polar cap area as derived from satellite images represents the magnitude of the open flux. Viking observations showed that the polar cap area was highly variable during the growth phase. While the equatorward boundary of the aurora near midnight was found to move consistently southward during the growth phase, the northern boundary would sometimes deviate poleward during its equatorward trend. The difference between the two boundary motions has been attributed to fading of high-latitude auroral activity [*Davis*, 1963] and the narrowing of the low-energy precipitation region [*Meng and Makita*, 1986]. From a global perspective these observations suggested that the polar cap would appear to expand because precipitation decreases below measurement levels or the auroral region thins in latitude, both of which need not be related to changes in the size of the open flux region.

With the deployment of the Ultraviolet Imager (UVI) [*Torr et al.*, 1995] on the Polar spacecraft it is now possible to investigate these issues on a global scale as the aurora borealis is observed for up to 6 to 8 hours at greater than 1-min resolution [*Brittnacher et al.*, 1997a]. Here we report a study of the relationship between polar cap area and substorm phase using UVI images for three events. The polar cap region was determined by an algorithm that selected regions poleward of the auroral oval that did not exceed a predetermined threshold. This is different from previous methods. *Frank and Craven* [1988] and *Kamide et al.* [1998] used a 1-kR (kilorayleigh) contour to define the polar cap boundary, and *Germany et al.* [1998] used a neural network boundary identification algorithm. These methods relied on determining a boundary for the polar cap. Our method sums regions devoid of precipitation that can have very irregular boundaries and are sometimes not enclosed in a single region. The reasons for choosing our threshold method are discussed in section 2. Changes in the polar cap area and in the poleward and equatorward boundary of the auroral oval were investigated in conjunction with measurements of solar wind IMF orientation and magnitude from the Wind spacecraft. Local time variations in the polar cap boundary were also studied using spacecraft image "keograms," a time series of luminosity across auroral latitudes for a fixed magnetic local time. These new global observations of the aurora are discussed below in the context of current models of the substorm growth and expansion phase.

2. Methods

Three substorm events in January 1997 were selected where UVI was able to monitor the entire auroral oval for several hours. The three events also occur for different IMF conditions and provide an opportunity to determine what may be common to substorms or vary with IMF magnitude and orientation. Boreal winter substorm events were chosen to avoid corrections for dayglow contamination. UVI images are recorded every 37 s using two filters that select the short (LBHs) and long (LBHl) wavelengths of the Lyman-Birge-Hopfield spectrum. The LBH spectrum is produced by electron impact excitation and is not susceptible to resonant scattering, quenching, or other processes that can modify the column-integrated intensity. Since Schumann-Runge absorption by O_2 is negligible for the longer wavelengths of the LBH spectrum, the luminosity observed at the spacecraft does not depend on the emission altitude or, consequently, the average energy of the precipitating electrons. Therefore the auroral luminosity observed with the LBHl filter is directly proportional to the energy flux of the precipitating electrons. The LBHl images, calibrated in units of photon flux, were converted to energy flux of precipitating electrons using auroral transport modeling [*Lummerzheim and Lilensten*, 1994; *Germany*, 1997] and then transformed into the Apex magnetic coordinate system [*Richmond*, 1995]. An emission altitude of 120 km is assumed in mapping the images. Only images using the LBHl filter are shown in this report, although all images were examined to determine substorm onset times.

For brevity, the region contained within the boundaries of auroral luminosity in this study will be designated simply as the "polar cap." However, this region is not necessarily equivalent to the region of open flux tubes that normally defines the polar cap. The polar cap region is determined by a statisically significant threshold of auroral luminosity measured in terms of a photon flux at the camera of 4 photons cm^{-2} s^{-1}. The minimum instrument sensitivity is about 0.5 photons cm^{-2} s^{-1}. This corresponds to a brightness of 120 R or, when converted to units of electron energy flux of the incident electrons, 1 erg cm^{-2} s^{-1}. All regions poleward of the auroral oval that are below this threshold are included in the polar cap region whereas oval-aligned arcs or theta aurorae structures are not. The particular value selected for the threshold was determined from data analysis issues—for instance determining where the edge of auroral luminosity rises above the noise level—but is guided by the general physics of the problem. Most polar cap precipitation, such as polar rain, has an energy flux of much less than 1 erg cm^{-2} s^{-1}, but large-scale arc structures in this region generally ex-

ceed this value. However, there is no sharp distinction in energy flux between precipitation on closed or open field lines, and therefore the choice of a threshold is, by necessity, arbitrary. The assumption implicit in the decision to exclude bright structures from the polar cap is that they most likely occur on closed field lines. For example, the detection of ions of plasma sheet origin in theta aurora arcs [*Peterson and Shelley*, 1984] suggests that these structures lie on closed field lines. A variety of polar cap arc structures have been observed, and interpretations of whether such structures occur on open or closed field lines vary [e.g., *Newell et al.*, 1997, and references therein]. During dynamic times when the magnetic topology is rapidly changing, the assumption that auroral precipitation occurs on closed field lines is also questionable [*Elsen et al.*, 1998]. Furthermore, the distinction between polar cap and auroral oval arcs cannot always be reliably made from the ultraviolet images. Some arc structures in the polar cap are connected to the oval, and it is not always apparent where to separate the two, or that the two really are distinct features [*Meng and Akasofu*, 1976; *Murphree and Cogger*, 1981; *Germany et al.*, 1998]. In this paper we use the terms oval-aligned and Sun-aligned to denote auroral structures in the polar cap that are slightly separated or completely separated from the auroral oval, respectively, in accordance with the discussion of *Murphree and Cogger* [1981]. The polar cap boundary is, in general, not a simple circle and sometimes consists of separate regions of open field surrounded by a closed field region [*Newell et al.*, 1997]. The threshold method does not distinguish auroral features on the basis of their latitude or orientation with respect to the oval; it simply eliminates all such structures from the polar cap. If there are closed field regions poleward of the observed auroral oval where there is no electron precipitation, or it is too weak to detect, including these regions as part of the polar cap will overestimate the open field region. In cases where sections of the oval disappear altogether or is below the predetermined threshold, which occur relatively often, a method is required to close the polar cap region. The method that is easiest to implement is curve-fitting across the missing region using the adjacent boundaries that are more clearly resolved in the images.

3. Observations

3.1. January 9, 1997

The six UVI images in Plate 1 show the progression of the aurora through the growth and expansion phases of the substorm. Between 0500 and 0700 UT the auroral precipitation was weak and sections of the oval were below the selected threshold value, as seen at 0534 and 0651 UT, altough most of the oval can still be resolved. At 0534 UT the brightest feature is a Sun-aligned structure while at 0651 UT the oval appears thinner and more distinct. A small brightening of the aurora, possi-

bly a pseudobreakup, is seen in the next image at 0719 UT. In the intervening 28 min the size of the oval had increased from about 8 to 10 $\times 10^6$ km^2, a 25% expansion. The polar cap area measurements are accurate to about 1×10^6 km^2 on the basis of statistical fluctuations in the measured values (standard deviation = 0.4 $\times 10^6$ km^2) and estimated error introduced by curve fitting across the gaps in the oval. Although the oval was weak and the polar cap region not well resolved, the expansion is statistically significant. It is also a simple geometrical fact that since the area of the roughly circular polar cap region is proportional to the square of the radius, small boundary motions can have a large effect on the area. Prior to the substorm a nominal 10 to 15 GW (1 gigawatt = 10^{16} erg s^{-1}) of power is transferred to the ionosphere in the auroral oval by electron precipitation, which is typical for a quiet period [*Brittnacher et al.*, 1997b]. By 0747 UT the auroral precipitation had increased, and the boundaries of the auroral oval at the end of the growth phase could be more clearly resolved. A small increase in electron precipitation in the presubstorm oval is a common feature observed in the UVI data set for all local times except near noon. Near apogee the dawn and dusk boundaries are accurate to 0.6° magnetic latitude (2 pixels, including the point spread function), and the high- and low-latitude boundaries near midnight and noon are exaggerated by about 1.5° (5 pixels) each, owing to spacecraft wobble that is aligned roughly along the noon-midnight meridian. Note that the polar cap area in Plate 1 had decreased by about 10% at the time of the pseudobreakup, seen as a 10-min-long bump in precipitation power. The area increased over the next 26 min and, at substorm onset, achieved its maximum at the same value as prior to the pseudobreakup, 10×10^6 km^2.

Within the 37 sec time resolution of UVI the substorm onset was first observed at 0747 UT as a brightening of the aurora in the 23.5 magnetic local time (MLT) region. Note how the auroral oval has become thinner and the polar cap boundary more distinct at 18 and 6 MLT. The rapid increase in precipitation at 0747 UT is followed by three intensifications which peak at 0759, 0818, and 0839 UT. The auroral activity at 0759 UT has spread in local time between 20 and 2 MLT and has expanded northward by 2° to 4° magnetic latitude (MLAT). By 0839 UT the polar cap has significantly contracted in size. Note the extreme high latitude to which the aurora has expanded in the 19 to 1 MLT region in spite of the fact that the peak intensity of the auroral precipitation is only 80 GW, a small substorm. Note also how the dayside portion of the auroral oval is missing, another feature common to substorms that is seen in all three events in this report. Following the substorm onset, the polar cap area decreased from 10×10^6 km^2 to 4.5×10^6 km^2 about 50 min later. Either a slowing of the increase or a decrease in the polar cap area occurs simultaneously with each of the three intensifications. That is, the decrease in the polar cap

area occurs at the same time as the auroral activity expands into the polar cap region. The expansion of the aurora to high latitude reduced the polar cap area by an amount that is nearly three times what was gained during the 25 min prior to the substorm. Although the substorm was relatively small in terms of total energy deposition by auroral precipitation, a significant reduction of the polar cap area occurred, mainly because of the nightside expansion. Neither the increase in the polar cap area nor its decrease were monotonic with time. The solar wind IMF plotted in GSM coordinates (used throughout this paper) in Plate 1 was measured by the Magnetic Fields Investigation (MFI) instrument on the Wind spacecraft [*Lepping et al.*, 1995] located at $(x, y, z)_{GSM} = (79, -60, 1)$ R_E. The propagation time was estimated to be about 17 min on the basis of a solar wind speed of approximately 430 km s^{-1} (not shown). The B_z component was never below -1 nT for 2 hours prior to the substorm and turned northward about 30 min before the onset as seen in Plate 1. The IMF was directed mainly toward Earth with a magnitude of about 6 nT. It may be that an increase (or decrease) in the solar wind dynamic pressure prior to this substorm (not shown) or $B_y \gg B_z$ triggered this event.

A more detailed analysis of the variation of the polar cap boundary with MLT was accomplished by constructing a "keogram" from UVI images, the magnetic latitudinal cross section of the aurora at a fixed MLT position plotted as a function of time, as seen in the bottom four panels in Plate 1. The resolution is one-half hour in MLT and one-half degree magnetic latitude. At local noon the latitudinal width of the aurora is quite broad, and the precipitation is weak (less than 2 erg cm^{-2} s^{-1}) and diffuse. The intensity seems to be the greatest between 75° and 78° magnetic latitude (includes ± 1.5° wobble error). The lower-latitude cutoff in the noon keogram is due to the edge of the field of view of the instrument. An adjustment of the despun platform position at 0700 UT moved the edge of the field of view to 71°, and it subsequently drifted to lower latitude. Between 0700 and 0840 UT the faint precipitation at noon moves about 1° to 2° equatorward. On the duskside the aurora at 18 MLT becomes more narrow and sharply defined beginning at about 0630 UT, and the precipitation at high latitude decreases below the level of detection. The aurora is 2° to 3° in width (no wobble error) and the equatorward boundary moves equatorward about 6° between 0640 and 0840 UT while the poleward boundary moves equatorward about 2° before expanding poleward. A keogram at the local time of the substorm onset, 23 to 23.5 MLT, reveals a 2° to 3° equatorward motion of the poleward and equatorward boundaries of a weak aurora before the pseudobreakup at 0719 UT. The poleward expansion of the aurora during the substorm begins at 0747 UT and continues for about 30 min, after which the poleward boundary remains at high latitude (about 81°, uncorrected for wobble) for more than an hour while the intensity fades. In

the 6 MLT region the oval boundaries were more distinct after 0650 UT coincident with the increase in the polar cap area. Note that after 0702 UT the edge of the UVI field of view is near the equatorward boundary of the oval and gradually drifts down in latitude. The intensity of the aurora between 70° and 75° decreases during the pseudobreakup at 0719 UT and during the second poleward motion beginning at 0804 UT. These decreases in intensity cause the poleward boundary of the more intense precipitation to fluctuate over a 5° range in latitude while the boundary of the less intense precipitation moves southward by only a few degrees. There is also a brightening of the aurora at lower latitude coincident with the second poleward expansion at 0805 UT that moves the lower boundary toward the equator by about 4°. In this case the slight decrease in latitude of the poleward boundary is due to a reduction of the lower intensity precipitation at the higher latitudes and a narrowing of the oval but not a shift of the oval to lower latitude. It appears that the increase in emissions between 65° and 70° MLAT at 0805 UT is the result of an increase in field-aligned current at lower latitude rather than a shift of the current system down in latitude since the poleward boundary concurrently moves slightly poleward.

3.2. January 10, 1997

During the first few hours of the magnetic cloud event on January 10, 1997, discussed by *Burlaga et al.* [1998] the polar cap contained many features at high latitude that were at times more intense than any region of the oval, as seen in Plate 2 at 0238 UT. These bright structures, discussed in detail by *Spann et al.* [1998], consisted of Sun- or oval-aligned arcs connected to the dawn and dusk flanks of the oval and irregular patches of precipitation, including intense emissions at the magnetic pole. The increase in the number, luminosity, and size of these structures between 0113 and 0238 UT leads to the decline in the polar cap area shown in Plate 2. Motion of the polar cap structures can be seen by comparison of the 0238 and 0245 UT images. The Sun-aligned arc in the high-latitude morning sector has moved toward the dusk. The clearing of the polar cap, which is complete at 0330 UT, proceeds by the "sweeping away" of polar cap structures from the high-latitude region. The center of the expansion away from which the structures appear to move is located on the morningside at about 80° MLAT. The IMF orientation, as recorded at the Wind spacecraft at $(x, y, z)_{GSM} = (85, -56, -20)$ R_E, was northward for at least an hour prior to 0225 UT and then turned southward over a few minutes and remained southward for about 45 min. Taking into account the propagation time to the magnetopause of about 18 min, on the basis of a solar wind speed of 440 km s^{-1} (not shown), the change in the trend of the polar cap area from contracting to expanding near 0240 UT occurs about 15 min after the southward turning of the IMF. The clearing of the polar cap contributed
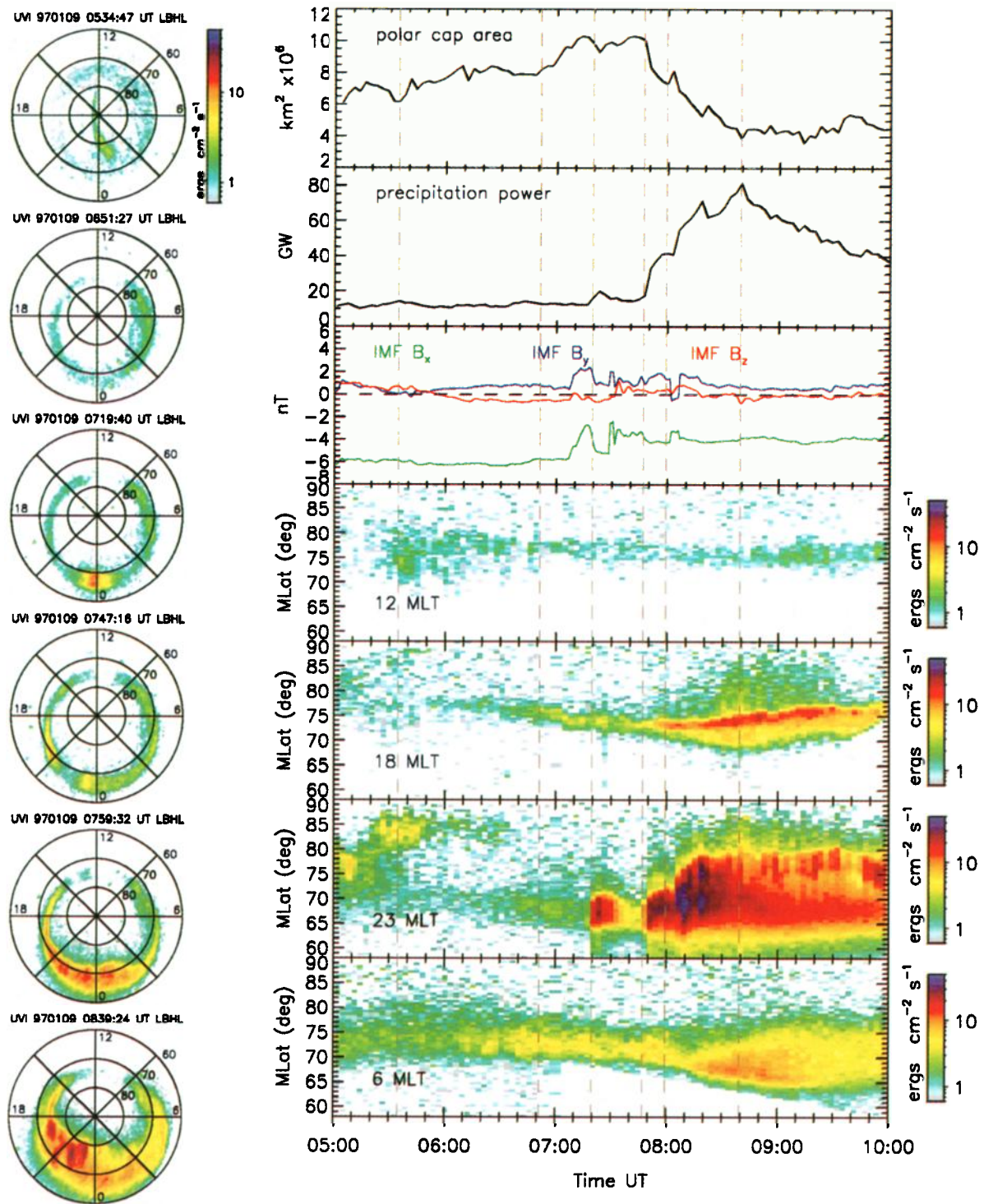
Plate 1. A selection of UVI images plotted in magnetic coordinates illustrates the auroral oval and polar cap dynamics during the growth and expansion phase of a substorm on January 9, 1997. The UT time at the beginning of the 37-s integration period is indicated in the image labels and by the vertical dashed lines in the series of panels on the right. The area of the polar cap, the total hemispheric electron precipitation power, and the auroral intensity versus time and latitude for 4 MLT locations (auroral "keograms") shown in the right series of panels are derived from the UVI images. The solar wind IMF components are corrected for propagation time to the magnetopause, estimated to be about 17 min.
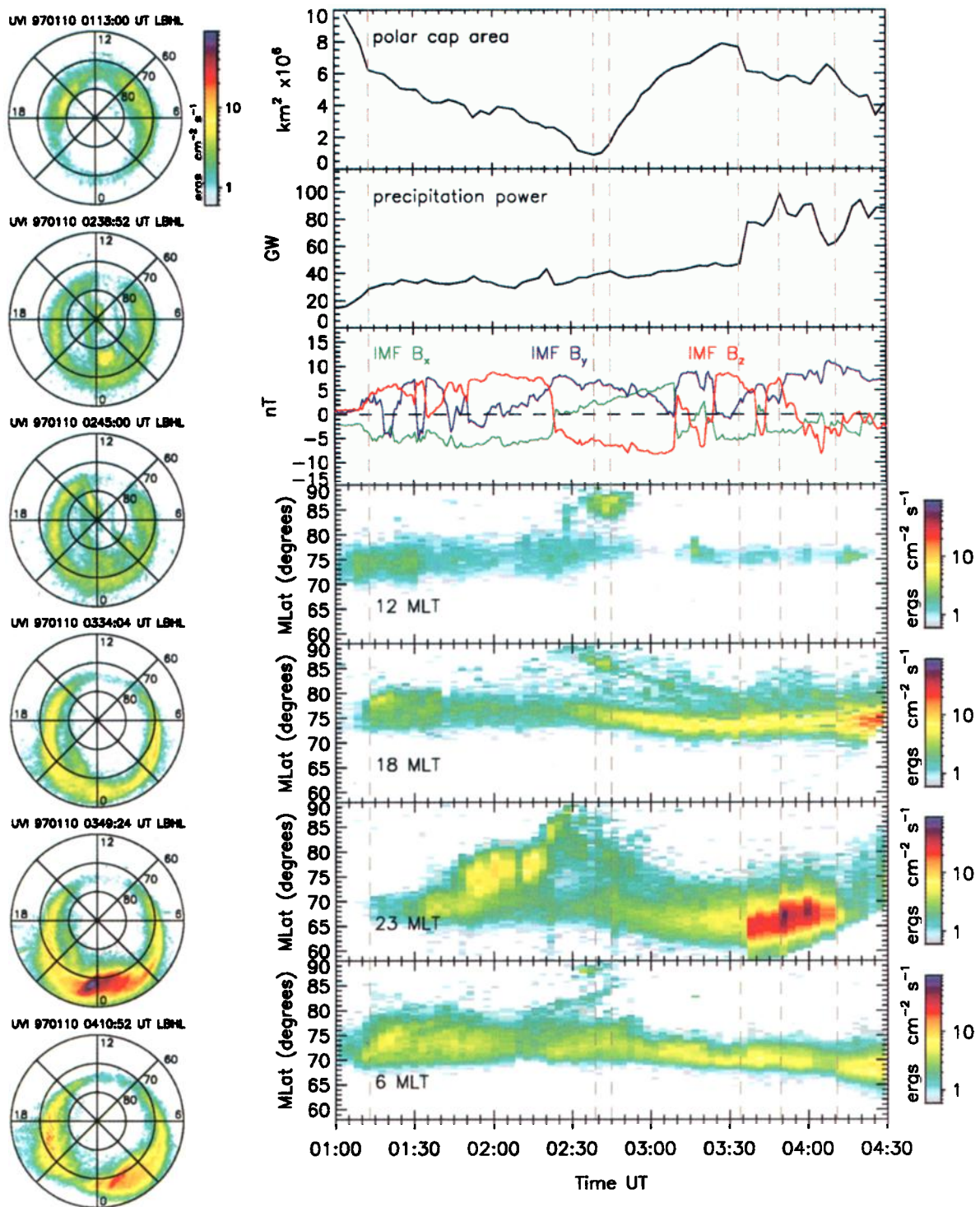
Plate 2. On January 10, 1997, complex auroral structures filled the polar cap during a period of predominantly northward IMF. The beginning of the clearing of the polar cap, seen by comparison of the 0238 and 0245 UT images, shows the "sweeping" of the arc structures toward the duskside of the high-latitude polar region. The large increase in the polar cap area during this period, shown in the top panel at the right, reflects the clearing of the polar cap by the motion and fading of the high-latitude arc structures following a southward turning of the IMF. During the substorm expansion, seen at 0349 UT, the duskside high-latitude arc structure remains and even brightens. The estimated solar wind propagation time to the magnetopause of about 18 min has been included.

toward the large and rather monotonic increase of the polar cap area during the 52 min between 0238 and 0330 UT. Some motion to lower latitude of the oval can be seen and will be discussed further in connection with the keogram below. No measureable increase or decrease in the polar cap area occurs during the 10 min prior to the substorm expansion. This may be due to the IMF turning northward; however, the uncertainty in the timing of the arrival of these changes in the solar wind and the polar cap area measurement makes this assertion difficult to verify. The timing of the substorm onset with respect to the northward turnings is similarly uncertain [*Spann et al.*, 1998]. There is an increase in total precipitation power in the hemisphere during the growth phase, as noted in the previous event. The dawnside and duskside oval has become thinner and more sharply defined, a feature that was also reported by *Spann et al.* [1998].

At 0334 UT the first brightening associated with the substorm is observed near 0 MLT. The maximum in the polar cap area is achieved near the time of the onset. The decrease in the polar cap area is coincident with a rapid rise in precipitation. A faint Sun-aligned arc can still be seen, and it persists even during the poleward expansion of the aurora at 0349 UT. This is due to the fact that the substorm expansion occurs simultaneously with rapidly changing B_y and B_z components that have been shown to be responsible for Sun-aligned arcs [*Cumnock et al.*, 1997; *Chang et al.*, 1998]. The poleward expansion at 0349 UT is shifted more to the dawnside than the January 9 event described above, probably because of the large positive B_y during this time as seen in Plate 2. Note also that the Sun-aligned arc on the duskside remains during the substorm expansion and even increases in intensity. However, for awhile it falls below the threshold for determining the polar cap and becomes included in the polar cap area estimate during this time. At 0410 a gap occurs in the aurora near 22 to 23 MLT. The occurrence of such gaps in the midnight oval has been analyzed by *Chua et al.* [1998]. The precipitation power show a slight increase during the 2 hours before onset and then rapidly rises following onset. The rapid rise is coincident with a decrease in polar cap area. The area continues to decrease during the auroral intensifications and it increases when the precipitation decreases. The poleward boundary for this substorm did not achieve as high a latitude as the January 9 event but was 6° to 7° lower in latitude, even though the two events are comparable in the total energy dissipated by electron precipitation.

All four of the keograms at 12, 18, 23.75, and 6 MLT in Plate 2 show the clearing of the polar cap or the retreat to lower latitude of the high-latitude structures between 0230 and 0330 UT, prior to the substorm onset. The equatorward boundary moves about 2° to 3° lower in latitude between about 0230 and 0310 UT near midnight and on the duskside. On the dawnside the equatorward boundary is steady until about 0300 UT and

then moves only about 1° to 2° lower in latitude before the substorm onset. Although the aurora near noon is weak, the equatorward boundary appears to move a few degrees lower in latitude between 0250 and 0310 UT. Together, these observations illustrate that the motion of the equatorward boundary is not correlated at all local times. Following the substorm onset, the equatorward boundary at 18 MLT moves poleward by a few degrees, while at 6 MLT it remains steady or moves southward by about 1°. The noon and midnight equatorward boundaries unfortunately fall outside of the UVI field of view at this time. The equatorward boundary on the dawnside moves to lower latitude more rapidly between 0410 and 0430 UT, making a total southward retreat of about 7°. Between 0240 and 0310 UT the peak in the auroral emissions moves down in latitude in all 4 keograms suggesting that the expansion of the oval is due to motion of the field-aligned current systems.

3.3. January 12, 1997

Although the beginning of the growth phase is not easy to determine from the plot of the polar cap area in Plate 3, a 40% increase over the 46-min period from 0635 to 0721 UT is evident. The oval at 0635 UT is broad and diffuse, and the polar cap is contracted. The remnants of high-latitude activity near 23 MLT are also apparent. The IMF was northward prior to this time, as seen in Plate 3, after correction for a propagation time to the magnetopause of about 18 min. At 0721 UT the activity near 23 MLT has subsided and the oval has become thinner with sharper and more distinct boundaries. The IMF orientation is characterized by continuously positive B_y, B_x fluctuating about 0, and strong southward B_z, except for a 5 min period of northward B_z beginning at 0712 UT. On the basis of a solar wind speed of about 450 km s^{-1} (not shown) the propagation time from the Wind spacecraft at $(x, y, z)_{GSM} = (103, -54, -9)$ R$_E$ to the magnetopause is estimated to be about 18 min. Using this estimate, the substorm onset occurs about 10 min after the northward turning arrives at the magnetopause. Prior to that the IMF had been mostly southward for about 40 min and it remained southward again after 0720 UT for nearly 80 min. Although the increase in area is comparable to what was observed on January 9, the polar cap area was already large at the beginning of the growth phase, and the maximum value achieved was the largest recorded for the three events we examined, 12×10^6 km^2.

The first sign of a substorm onset appears in the 23-MLT region at 0724 UT. The polar cap area achieves its maximum value at the time of onset, and again at 0758 UT. This behavior is different from that observed in the previous two events in that the polar cap area recovered to its maximum value. Four distinct intensifications of the substorm were observed with maximum values of precipitation energy achieved at 0734, 0750, 0810, and
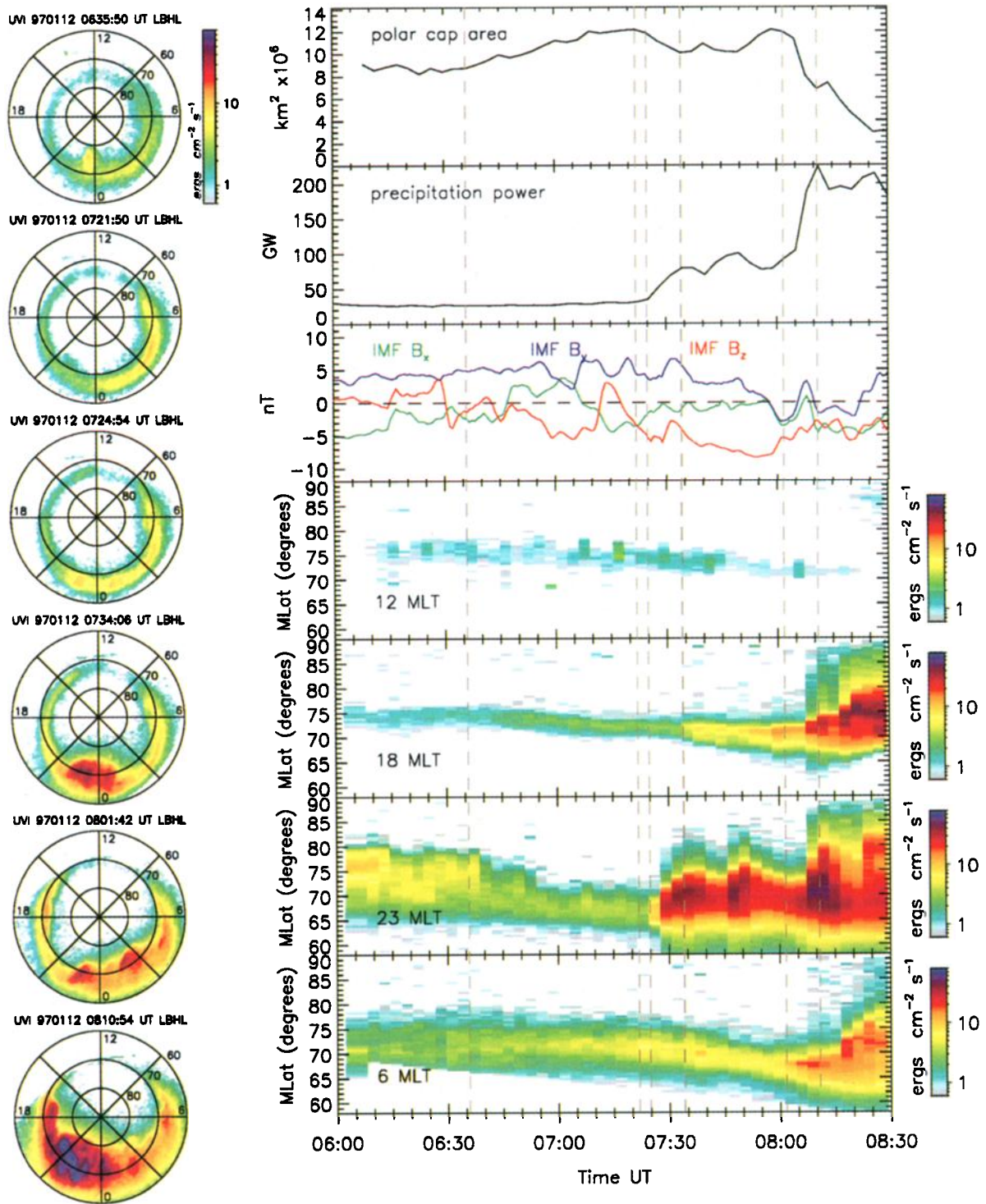
Plate 3. On January 12, 1997, the fading of previous high-latitude activity in the midnight region concurrent with the general expansion of the oval at all local times, except the dawnside, for about 1 hour prior to onset of a substorm produces a gradual increase in the polar cap area. Each of the intensifications peaking at 0734, 0750, 0810, and 0827 UT reduce the polar cap area, although increases in polar cap area also occur during the substorm. The dusk boundary at 18 MLT remains steady during the substorm onset while the dawnside decreases in latitude 15 minutes after onest. At midnight rapid poleward expansions and gradual recoveries are seen for each intensification of the aurora. The high-latitude expansion of the aurora is similar to what was observed for the much smaller substorm on January 9, 1997, shown in Plate 1. The estimated solar wind IMF propagation time is about 18 min.

0827 UT. The first two were relatively small but comparable to the values obtained during the January 9 and 10 events. The poleward expansion of the aurora in the 23-MLT region during the first intensification did not achieve as high a latitude as did the substorm on January 9, although the total energy precipitated was roughly equivalent. Prior to the the second intensification peaking at 0750 UT a small but statistically significant increase in the polar cap area is evident. During the second intensification the polar cap area again decreases, but then rapidly rises back to its maximum value at 0758 UT. Note that the IMF had turned southward during the substorm and may account for the increase in the polar cap area during the expansion. The nightside aurora during the third and much larger intensification expands to roughly 85° MLAT, a few degrees higher value than was observed during the January 9 event, albeit for a much less intense substorm. The further decrease in the polar cap area during the fourth intensification at 0827 UT is partly due to the dayside oval moving out of the UVI field of view beginning at 0820 UT and the inability of the algorithm to create a reasonable boundary for so large a gap in the oval.

The keogram for 18 MLT in Plate 3 shows that the polar cap boundary decreases only about 1° MLAT prior to the substorm onset and does not begin to move poleward until the strongest intensification of the aurora at 0805 UT. At 23 MLT the polar cap boundary shows a more remarkable equatorward retreat of nearly 10° MLAT prior to onset, a rapid poleward expansion of 10° in the next 10 min, and then a slight recovery. The second, third, and fourth intensifications of the aurora also show the same behavior of a rapid poleward expansion followed by a slower recovery at 0745, 0805, and 0820 UT. The polar cap boundary at 6 MLT is steady prior to onset and declines in latitude for 30 min following the onset. This corresponds to a period of negative B_z and is evidence of latitudinal motion of the oval in response to a southward orientation of the IMF. At 0805 UT, when the precipitation rapidly increases at this local time, the decline in latitude of the poleward boundary stops and then reverses to expand poleward rapidly while the equatorward boundary continues to move to lower latitude.

4. Discussion

The polar cap region during the substorm growth phase was consistently found in this study to expand in size, independent of the magnitude of the IMF B_z component. The increase in the polar cap area was observed to last from 30 to 50 min. The increase in the area was as little as 25% or as much as a fourfold increase, as seen on January 10 when the polar cap was filled with considerable activity before the substorm. There were three phenomena that contributed toward the increase in the polar cap region: (1) motion of the auroral oval to lower latitude, (2) the decrease in latitudinal width

(thinning) of the auroral oval, and (3) clearing of the polar cap of intense auroral precipitation. These mechanisms did not always act concurrently or equivalently at all local times. This suggests that they are not related to each other in terms of their physical cause. However, they all occurred during the substorm growth phase.

The motion of the auroral oval to lower latitude during the substorm growth phase contributed toward, but did not account for, the entire change in the polar cap area. The equatorward motion of the poleward and equatorward boundaries of the auroral oval did not consistently move together. More often, the poleward boundary would evidence a more rapid equatorward motion than the equatorward boundary. The motion of the more intense aurora appeared to follow the slower equatorward motion of the equatorward boundary. This suggests that a shift of the field-aligned currents system took place, but more likely at the slower pace indicated by the equatorward boundary. The rapid motion of the poleward boundary is related to thinning of the auroral oval and the clearing of the polar cap (discussed more fully below). Current models of the substorm phase predict that the expansion of the polar cap region is due to the increased rate of merging of the solar wind magnetic field with the dayside magnetopause. The decrease in magnetic latitude of a few degrees on the dayside and about 3° to 4° on the nightside observed in this study is consistent with this model. However, what is not consistent with the model is that the shift to lower latitude did not take place concurrently at all local times, an observation also reported by *Kamide et al.* [1998]. The asymmetry between the dawn and dusk oval motion can arise from IMF B_y orientation, differences in conductivity that influence the location of the field-aligned and ionospheric currents surrounding the polar cap, and other factors that determine the polar cap boundary.

The decrease in latitudinal width of the auroral oval increased the polar cap area because it occasionally occurred without a decrease in latitude of the auroral oval or the poleward boundary moved more rapidly than the equatorward boundary to lower latitude. During quiet times or northward IMF the width of the oval generally broadens [*Meng*, 1981]. The decrease in latitudinal width of the oval may be associated with the thinning of the plasma sheet, commonly observed during the substorm growth phase [*Sergeev et al.*, 1990; *Sanny et al.*, 1994]. The thinning of the plasma sheet has typically been observed for southward IMF. Increases in the polar cap area during periods of southward IMF were noted in the January 10 and 12 events and have also been reported previously [e.g., *Meng and Makita*, 1986; *Frank and Craven*, 1988; *Germany et al.*, 1998]. However, on January 9, 1997, the oval as seen at the time of the substorm onset is quite thin, even though the IMF B_z component was 0 ± 0.5 nT. The earthward oriented IMF on January 9 caused nearly the same increase in the polar cap area as observed on January 12

during a large southward oriented IMF. Thus the IMF control of the polar cap area is not entirely dependent upon the magnitude of the IMF B_z component. This is unexpected according to the current substorm model, which predicts that a large southward IMF should be more effective in the production of open flux in the polar cap than other orientations of the IMF for a given total magnitude of B.

The more interesting and least understood mechanism of increasing the polar cap area is the clearing of the polar cap of precipitation. The January 10, 1997, event is a very dramatic illustration of this feature. There were numerous Sun-aligned arc structures at high latitude, which is typical of relatively quiet times and northward IMF conditions. When the IMF turned southward, the high-latitude region cleared of precipitation, but this process took as long as 30 min. During this event, polar cap arc structures appear to be swept away by both their motion and decrease in intensity. This phenomenon may be similar to the decrease in polar cap arcs with increasing auroral electroject activity reported by *Davis* [1963], on the basis of all-sky camera observations. From a global point of view the entire polar cap region becomes devoid of precipitation, although weak remnants of oval-aligned arcs can remain during a substorm, as seen during the January 10 event. There are no models that currently predict this phenomenon, although current models of field line merging provide part of the explanation for this feature. For instance, the motion of the dawnside arc away from the dawnside oval (Plate 2) was suggested by *Newell et al.* [1998] to be the result of convection of newly opened flux tubes from a dayside reconnection site. Dayside merging alone cannot provide the entire explanation for the clearing of the polar cap because the Sun- or oval-aligned arc structures in the polar cap are not completely swept out of the polar cap, as observed on January 10. However, the level of precipitation in the polar cap has considerably decreased. Concurrent with the clearing of the polar cap, it was also noted that the precipitation in the oval increased, another feature typical of the growth phase found in UVI observations. Since there is an overall increase in the precipitation power in the entire hemisphere, the brightening of the auroral oval cannot be accounted for by simply transferring the polar cap precipitation to the oval. Therefore a process different from the opening of flux tubes to the solar wind is causing the precipitation in the polar cap arcs to fade in intensity during the growth phase; otherwise, these features would disappear altogether from the polar cap or be combined with the dawn or dusk oval. Also, the polar cap arc seen on January 10 brightens following the substorm onset, indicating that its source region is most likely the plasma sheet. The cause of the fading may be a reduction of the field-aligned electric field in the polar cap. The oval-aligned arc region was included in the polar cap by our algorithm because it faded below the threshold of 1 erg cm^{-2} s^{-1} but was

most likely on closed field lines. Therefore the size of the polar cap is overestimated in this case.

Immediately following the substorm onset (or pseudo-breakup), the polar cap area was consistently observed to decrease, although later increases in the polar cap area during the substorm were found. The total decrease varied by as little as a factor of 2 and, for the case of January 12, 1997, the area decreased from 9 to 1×10^6 km^2. The precipitation in the high-latitude region within a few hours of midnight during the substorm expansion strongly controls the decrease in the polar cap area. It was noted that the polar cap area decreased concurrent with, and approximately in proportion to, the rise in electron precipitation during substorm activity. This anticorrelation between the polar cap area and the global electron precipitation power was not observed at times other than during a rapid increase in auroral activity. It was not always the case that contraction of the polar cap and increase in latitude of the poleward boundary were correlated. For example, during the January 12 substorm the polar cap area decreased at the same time as the poleward boundary between 6 and 12 MLT continued to move to lower latitude. This was during a strong B_z southward condition. Therefore the auroral oval motion near dawn and noon provides evidence of a response to solar wind IMF conditions during the substorm. This evidence of an increase in the oval at certain local times during the first 35 min of the substorm also indicates why the polar cap area did not decrease as much as the other two substorms in this study, and even returned to its value at the time of the substorm onset. *Kamide et al.* [1998] predicted that the polar cap region might not contract during the expansion phase for all substorms. In their view, competition between processes that add flux (e.g., dayside reconnection) and ones that extract flux (e.g., tail reconnection) from the polar cap might not always favor the latter process as the most significant. This is consistent with the fact that the polar cap area returned to its substorm onset size about 35 min later, during the strong southward IMF B_z. However, the polar cap area initially decreased following the substorm onset, indicating that the process responsible for controlling the poleward boundary of the aurora in the expansion region operated on a shorter timescale than the process that expanded the polar cap globally. It is also notable that the jump to high latitude of the nightside polar cap boundary during the expansion phase of the January 9 and 12 substorms reduced the polar cap area by 2 to 3 times the area gained during the growth phase. If these auroral emissions that expand into the polar cap are considered to be on flux tubes that close in the magnetosphere, and the reduction of the polar cap area is interpreted as a loss of open flux in the polar cap, then the current paradigm of substorm energetics would lead to conflicting conclusions for the two substorms. During both of these substorms the gain in area prior to onset was similar, as was the factor of 2 to 3 larger loss in

area following onset. However, the energy deposition for the January 12 substorm was more than twice as great. This implies that the gain or loss of area is not directly related to the magnitude of the substorm. This is contrary to the current substorm paradigm where particle energization is a byproduct of the conversion of open to closed flux by reconnection. A more direct relationship between the loss of polar cap area and the intensity of the substorm would be expected.

In summary, we have found that three processes, decrease in latitude of the poleward boundary of the oval, thinning of the oval, and clearing the polar cap of precipitation, contribute to the increase in the apparent size of the polar cap, and these processes can occur independent of the magnitude of the IMF B_z component. Not all of these features can be explained by current substorm models, and they provide new evidence of growth phase processes. Although we might want to know the fractional contribution of each of the three processes to the increase in the size of the polar cap, it is not always apparent how to distinguish their effects. We consider that the dynamics of the polar cap region during substorms may not be fully understood and that interpretation of changes in the polar cap area, as determined from auroral images, according to the current substorm paradigm might be misleading. For this reason we do not offer any estimates of the amount of magnetic flux gained or lost during substorms on the basis of the polar cap area. Such an excercise appears meaningless until we can more fully understand what we are observing in the global auroral images.

References

Akasofu, S.-I., and Y. Kamide, Substorm energy, *Planet. Space Sci.*, *23*, 223, 1975.

Baker, D. N., T. I. Pulkkinen, R. L. McPherron, and C. R. Clauer, Multispacecraft study of a substorm growth and expansion phase features using a time-evolving field model, in *Solar System Plasmas in Space and Time, Geophys Monogr. Ser.*, vol. 84, edited by J. L. Burch and J. H. Waite Jr., pp. 101-110, AGU, Washington, D. C., 1994.

Baker, D. N., T. I. Pulkkinen, M. Hesse, and R. L. McPherron, A quantitative assessment of energy storage and release in the Earth's magnetotail, *J. Geophys. Res.*, *102*, 7159, 1997.

Brittnacher, J. Spann, G. Parks, and G. Germany, Auroral observations by the Polar Ultraviolet Imager (UVI), *Adv. Space Res.*, *20(4/5)*, 1037, 1997a.

Brittnacher, M., R. Elsen, G. Parks, L. Chen, G. Germany, and J. Spann, A dayside auroral energy deposition case

study using the Polar Ultraviolet Imager, *Geophys. Res. Lett.*, *24*, 991, 1997b.

Burlaga, L., et al., A magnetic cloud containing prominence material: January 1997, *J. Geophys. Res.*, *103*, 277, 1998.

Chang, S.-W., et al., A comparison of a model for the theta aurora with observations from Polar, Wind, and SuperDARN, *J. Geophys. Res.*, *103*, 17,367, 1998.

Chua, D., M. Brittnacher, G. Parks, G. Germany, and J. Spann, A new auroral feature: The nightside gap, *Geophys. Res. Lett.*, *25*, 3747, 1998.

Craven, J. D., and L. A. Frank, Latitudinal motions of the aurora during substorms, *J. Geophys. Res.*, *92*, 4565, 1987.

Cumnock, J. A., J. R. Sharber, R. A. Heelis, M. R. Hairston, and J. D. Craven, Evolution of the gloval aurora during positive IMF B_z and varying IMF B_y conditions, *J. Geophys. Res.*, *102*, 17,489, 1997.

Davis, T. N., Negative correlation between polar-cap visual aurora and magnetic activity, *J. Geophys. Res.*, *68*, 4447, 1963.

Elphinstone, R. D., K. Jankowska, J. S. Murphree, and L. L. Cogger, The configuration of the auroral distribution for interplanetary magnetic field B_z northward, 1, IMF B_x and B_y dependencies as observed by the Viking satellite, *J. Geophys. Res.*, *95*, 5791, 1990.

Elsen, R. K., et al., The auroral oval boundaries on January 10, 1997: A comparison of global magnetospheric simulations with UVI images, *Geophys. Res. Lett.*, *25*, 2585, 1998.

Frank, L. A., and J. D. Craven, Imaging results from Dynamics Explorer 1, *Rev. Geophys.*, *26*, 249, 1988.

Gary, J. B., L. J. Zanetti, B. J. Anderson, T. A. Potemra, J. H. Clemmons, J. D. Winningham, and J. R. Sharber, Identification of auroral oval boundaries from in situ magnetic field measurements, *J. Geophys. Res.*, *103*, 4187, 1998.

Germany, G. A., G. K. Parks, M. Brittnacher, J. Cumnock, D. Lummerzheim, J. F. Spann, L. Chen, P. G. Richards, and F. J. Rich, Remote determination of auroral energy characteristics during substorm activity, *Geophys. Res. Lett.*, *24*, 995, 1997.

Germany, G. A., G. K. Parks, H. Ranganath, R. Elsen, P. G. Richards, W. Swift, J. F. Spann, and M. Brittnacher, Analysis of auroral morphology: Substorm precursor and onset on January 10, 1997, *Geophys. Res. Lett.*, *25*, 3053, 1998.

Kamide, Y., S. Kokubun, L. F. Bargatze, and L. A. Frank, The size of the polar cap as an indicator of substorm energy, *Phys. Chem. Earth (C)*, *24(1-3)*, 119, 1999.

Lassen, K., and C. Danielsen, Distribution of auroral arcs during quiet geomagnetic conditions, *J. Geophys. Res.*, *94*, 2587, 1989.

Lepping, R. P., et al., The Wind magnetic field investigation, *Space Sci. Rev.*, *71*, 207, 1995.

Lummerzheim, D., and J. Lilensten, Electron transport and energy degradation in the ionosphere: Evaluation of the numerical solution, comparison with laboratory experiments and auroral observations, *Ann. Geophys.*, *12*, 1039, 1994.

Makita, K., C.-I. Meng, and S.-I. Akasofu, Temporal and spatial variations of the polar cap dimension inferred from the precipitation boundaries, *J. Geophys. Res.*, *90*, 2744, 1985.

Meng, C.-I., Polar cap arcs and the plasma sheet, *Geophys. Res. Lett.*, *8*, 273, 1981.

Meng, C.-I., and S.-I. Akasofu, The relation between the polar cap auroral arc and the auroral oval arc, *J. Geophys. Res.*, *81*, 4004, 1976.

Meng, C.-I., and K. Makita, Dynamic variation of the po-

lar cap, in *Solar Wind-Magnetospheric Coupling*, edited by Y. Kamide and J. A. Slavin, pp. 605-631, Terra Sci., Tokyo, 1986.

Meng, C.-I., R. H. Holzworth, and S.-I. Akasofu, Auroral circle: Delineating the poleward boundary of the quiet auroral belt, *J. Geophys. Res.*, *82*, 164, 1977.

Murphree, J. S., and L. L. Cogger, Observed connections between apparent polar cap features and the instantaneous oval, *Planet. Space Sci.*, *29*, 1143, 1981.

Murphree, J. S., R. D. Elphinstone, L. L. Cogger, and D. Hearn, Viking optical substorm signatures, in *Magnetospheric Substorms, Geophys. Monogr. Ser.*, Vol. 64, edited by Kan et al., pp. 241-255, AGU, Washington D. C., 1991.

Newell, P. T., D. Xu, C.-I. Meng, and M. G. Kivelson, Dynamical polar cap: A unifying approach, *J. Geophys. Res.*, *102*, 127, 1997.

Newell, P. T., K. Liou, C.-I. Meng, M. Brittnacher, and G. Parks, Dyanmics of double-theta aurora: Polar UVI study of January 10-11, 1997, *J. Geophys. Res.*, in press, 1998.

Peterson, W. K., and E. G. Shelley, Origin of the plasma in a cross-polar cap auroral feature (theta aurora), *J. Geophys. Res.*, *89*, 6729, 1984.

Richmond, A. D., Ionospheric electrodynamics using magnetic apex coordinates, *J. Geomagn. Geoelectr.*, *47*, 191, 1995.

Russell, C. T., and R. L. McPherron, The magnetotail and substorms, *Space Sci. Rev.*, *11*, 111, 1973.

Sanny, J., R. L. McPherron, C. T. Russell, D. N. Baker, T. I. Pulkkinen, and A. Nishida, Growth-phase thinning of the near-Earth current sheet during the CDAW 6 substorm, *J. Geophys. Res.*, *99*, 5805, 1994.

Sergeev, V. A., P. Tanskanen, K. Mursula, A. Korth, and R. C. Elphic, Current sheet thickness in the near-Earth plasma sheet during substorm growth phase, *J. Geophys. Res.*, *95*, 3819, 1990.

Siscoe, G. L., and T. S. Huang, Polar cap inflation and deflation, *J. Geophys. Res.*, *90*, 543, 1985.

Spann, J. F., M. Brittnacher, R. Elsen, G. A. Germany, and G. K. Parks, Initial response and complex polar cap structures of the aurora in response to the January 10, 1997 magnetic cloud, *Geophys. Res. Lett.*, *25*, 2577, 1998.

Torr, M. R., et al., A far ultraviolet imager for the international solar-terrestrial physics mission, *Space Sci. Rev.*, *71*, 329, 1995.

Troshichev, O. A., E. M. Shishkina, C.-I. Meng, and P.T. Newell, Identification of the poleward boundary of the auroral oval using characteristics of ion precipitation, *J. Geophys. Res.*, *101*, 5035, 1996.

M. Brittnacher, M. Fillingim, and G. Parks, Geophysics Program, Box 351650, University of Washington, Seattle, WA 98195. (britt@geophys.washington.edu)

G. Germany, CSPAR, University of Alabama at Huntsville, Huntsville, AL 35807

J. Spann, NASA Marshall Space Flight Center, Huntsville, AL. 35812